Supplementary material (ESI) for Journal of Materials Chemistry

Supporting Information

Very High-Efficiency Red-Electroluminescence Devices Based on an Amidinate-Ligated Phosphorescent Iridium Complex

Tai Peng,[a] Hai Bi,[a] Yu Liu,*[,a] Yan Fan,[a] Hongze Gao,[a] Yue Wang,[a] and Zhaomin Hou*[,b]

[a]State Key Laboratory of Supramolecular Structure and Materials, Jilin University, Changchun 130012 (P. R. China)
E-mail: (yuliu@jlu.edu.cn)
[b]Organometallic Chemistry Laboratory, RIKEN Advanced Science Institute, 2-1 Hirosawa, Wako, Saitama 351-0198 (Japan)
E-mail: (houz@riken.jp)

Synthesis: Materials obtained from commercial suppliers were used without further purification. Anhydrous hexane was distilled with sodium benzophenone ketyl under nitrogen atmosphere, degassed by the freeze-pump-thaw method. All glass wares, syringes, magnetic stirring bars and needles were dried in a convection oven at least 4 hours. Reactions were monitored with thin layer chromatography (TLC). Commercial TLC plates (Silica gel 60 F254, Merck Co.) were developed and the spots were seen under UV light at 254 and 365 nm. Silica column chromatography was done with silica gel 60 G (particle size 5~40 μm, Merck Co.). ^{1}H NMR spectrum was recorded on a Bruker AVANVE 300 MHz spectrometer with tetramethylsilane as an internal standard. Mass spectra were measured on a GC/MS mass spectrometer. Elemental analyses were performed on a flash EA 1112 spectrometer.

(bt)$_2$Ir(dipba). In a 50-mL flask, a hexane solution of n-BuLi (0.15 mL x 2.6 M) was added to 1-bromobenzene (65 mg, 0.4 mmol) in hexane (10 mL) under argon. The reaction mixture was stirred at room temperature for 1 hour, and was then added dropwise to *N*,*N'*-diisopropylcarbodiimide (50 mg, 0.4 mmol). The colorless solution was stirred rapidly for 30 min, and then added dropwise to $[(bt)_2Ir(\mu\text{-}Cl)]_2$ (0.2 mmol, 265 mg) in hexane solvent (15 mL). After being stirred at 80℃ for 8 hours, the reaction mixture was cooled to room temperature. The solvent was evaporated under vacuum, and the product was washed with Et_2O (20 mL) three times, giving rise to (bt)$_2$Ir(dipba) (46%). MS: *m/z* 816 (M^+). Anal. Calcd for $C_{39}H_{35}IrN_4S_2$: C, 57.40; H, 4.32; N, 6.87. Found: C, 57.47; H, 4.35; N, 6.98. ^{1}H NMR (300 MHz, $CDCl_3$) δ 9.20 (d, J=8.1 Hz, 2H), 7.94 (d, J=7.8 Hz, 2H), 7.62-7.67 (m, 4H), 7.52 (t, J=7.8 Hz, 2H), 7.29-7.36 (m, 3H), 7.18 (d, J=6.9 Hz, 2H), 6.78 (t, J=7.8 Hz, 2H), 6.60 (t, J=7.5 Hz, 2H), 6.47 (d, J=7.8 Hz, 2H), 3.36 (m, 2H), 0.58 (d, J=6.3 Hz, 6H), -0.17 (d, J=6.3 Hz, 6H); ^{13}C NMR ($CDCl_3$) δ 180.40, 174.84, 156.39, 151.50, 140.91, 137.37, 133.50, 131.45, 130.14, 128.18, 127.95, 127.88, 126.32, 125.45, 124.99, 122.40, 122.34, 119.86, 47.36, 25.25, 23.81.

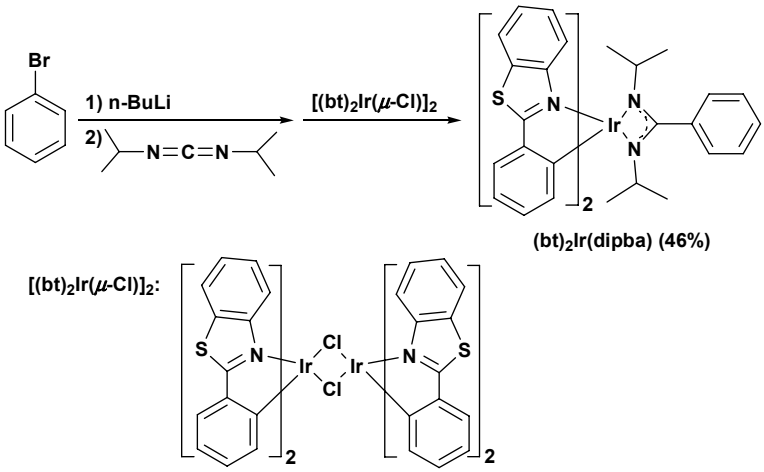

S-Scheme 1. Synthetic route for the Ir-complex **(bt)$_2$Ir(dipba)**.

***Absorption, PL and Electrochemical Measurements*:** Absorption spectra were obtained using a Shimadzu UV-2550 UV-vis spectrometer. PL spectra were recorded by a Perkin-Elmer LS-55 fluorescence spectrometer with a Xe arc lamp excitation source. Electrochemical measurements were performed with a BAS 100W Bioanalytical electrochemical work station, using Pt working electrode, platinum wire as auxiliary electrode, and a porous glass wick Ag/Ag^+ as reference electrode, standardized against ferrocene/ferrocenium couple, scan rate 100 mV s^{-1}.

The absorption spectrum of the iridium complex (bt)$_2$Ir(dipba) in degassed dichloromethane was shown in S-Fig. 1 The strong absorption bands below 360 nm can be assigned to spin-allowed $^1\pi$-π^* transitions on the cyclometalated ligands. The broad absorption bands at lower energies are typical for (metal-ligand charge transfer) ^{1}MLCT and ^{3}MLCT.

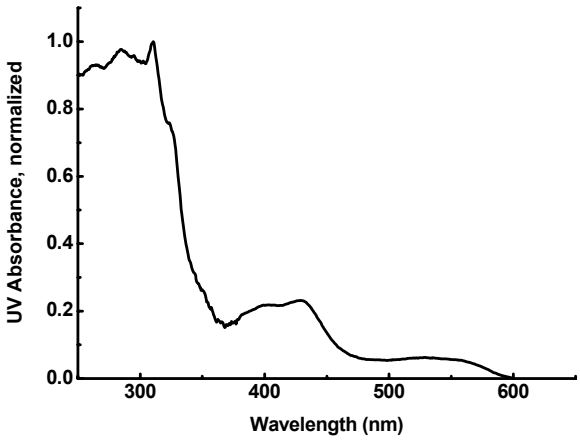

S-Fig. 1 UV-Vis absorption spectrum of **(bt)$_2$Ir(dipba)** in dichloromethane.

***Fabrication of the OLEDs and EL Measurements*:** The general architecture of the complex multilayer diodes used in this study is as follows: The ITO (indium-tin oxide) coated glass substrates (20Ω/square) were first cleaned in ethanol, acetone, and soap ultrasonic bathes. All organics were purified by gradient sublimation and thermally evaporated at a rate of 1.0 Å s^{-1} at a base pressure of around 3.5 x 10^{-4} Pa. A LiF layer (0.5 nm) was deposited at a rate of 0.2 Å S^{-1}. The finishing Al electrode (cathode) was deposited at a rate of 10 Å S^{-1} in another chamber. The active area of the diode segments was 2 x 3 mm^2. EL spectra and brightness-current density-voltage characteristics of the devices were measured by combining a Spectrascan PR-650 spectrophotometer with a computer-controlled direct-current power supply Keithley model 2400 voltage-current source under ambient condition at room temperature.

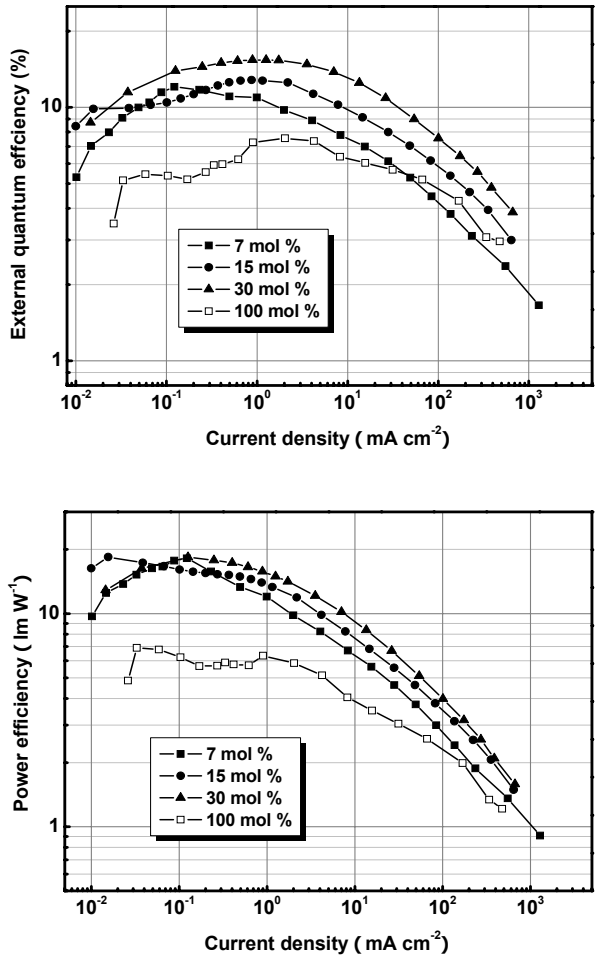

S-Fig. 2 (Top) External quantum efficiency-current density curves of devices I (7 mol %), II (15 mol %), III (30 mol %) and IV (100 mol %). (Bottom) Power efficiency-current density curves of devices I-IV.

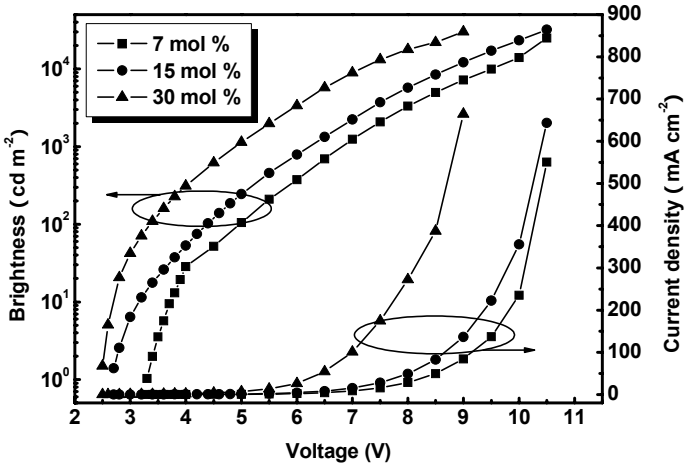

S-Fig. 3 Current density-brightness-voltage curves of device I (7 mol %), II (15 mol %), and III (30 mol %).

DFT Calculations: the ground-state was fully optimized by the DFT[S1] method with Becke's three-parameter functional and the Lee-Yang-Parr functional[S2] (B3LYP). In the calculations, "Double-ζ" quality and polarization basis sets were employed for the ligands (6-31G(d)) and the Ir (LANL2DZ). A relativistic effective core potential (ECP) on Ir[S3] replaced the inner core electrons leaving the outer core $[(5s)^2(5p)^6]$ electrons and the $(5d)^6$ valence electrons of Ir(III). On the basis of the optimized ground-state, the absorption property in dichloromethane (CH_2Cl_2) media was calculated by time-dependent DFT (TDDFT)[S4] associated with the polarized continuum model (PCM).[S5] This kind of theoretical approach has been proven to be reliable for transition-metal complex systems.[S6] All of the calculations were accomplished by using the Gaussian 03 software package.[S7]

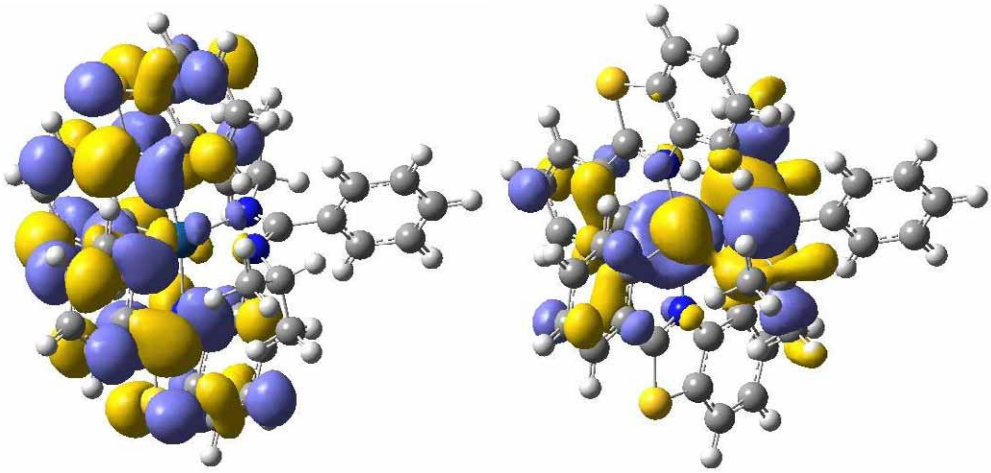

S-Fig. 4 The contour plots of LUMO (left) and HOMO (right) in **(bt)$_2$Ir(dipba)** from DFT calculations.

S-Table 1. Molecular orbital compositions (Percent) in the ground state for **(bt)$_2$Ir(dipba)** at the B3LYP.

	Orb.	Ir			bt				bt			dipba			
Orb.	Energy (eV)	sp	d	ben	total	N	S	ben	total	N	S	total	N	N	ben
183	0.24	0.6	2.5	8.3	39.3	3.9	0.1	8.3	39.1	3.8	0.1	1.9	0.2	0.2	1.2
182	0.22	1.0	1.2	5.7	41.9	1.8	18.1	5.8	42.1	1.8	18.1	2.2	0.3	0.3	1.1
181	0.16	1.6	1.5	6.6	37.7	1.9	13.8	6.6	37.7	1.9	13.8	8.3	0.7	0.7	6.4
180	0.02	1.1	9.6	2.3	42.0	1.2	28.7	2.3	42.0	1.2	28.7	0.7	0.1	0.1	0.3
179	-0.12	0.0	0.0	0.0	0.6	0.0	0.1	0.0	0.6	0.0	0.1	98.7	0.0	0.0	95.5
178	-0.29	0.6	0.1	0.2	51.2	0.0	2.4	0.1	46.3	0.0	2.2	1.5	-0.1	-0.1	0.9
177	-0.29	0.7	0.8	2.0	29.8	0.0	1.4	2.0	34.6	0.0	1.6	30.3	0.4	0.3	27.7
176	-0.34	2.3	1.3	0.7	17.7	0.0	0.7	0.7	17.7	0.0	0.7	59.6	2.1	2.1	50.2
175	-1.51	0.2	3.2	15.5	32.3	5.3	3.7	15.5	32.3	5.3	3.7	1.0	0.3	0.3	0.1
174(LUMO)	-1.66	1.0	1.4	**16.9**	**31.4**	5.6	4.0	**16.9**	**31.4**	5.6	4.0	1.1	0.2	0.2	0.3
173(HOMO)	-4.69	0.9	**24.7**	5.5	2.1	0.6	0.1	5.5	2.1	0.6	0.1	**59.2**	**24.5**	**24.5**	0.2
172	-5.16	0.7	30.0	17.6	4.1	0.9	1.0	17.6	4.1	0.9	1.0	26.1	10.5	10.5	0.1
171	-5.53	0.1	42.9	11.7	13.5	4.1	0.2	11.7	13.4	4.1	0.2	6.8	0.9	0.9	0.9
170	-5.80	0.5	32.1	12.2	16.2	4.1	1.0	12.2	16.2	4.1	1.0	10.5	4.0	4.0	0.5
169	-6.00	0.0	20.8	24.0	12.0	0.5	4.3	24.0	12.0	0.5	4.3	7.1	1.2	1.2	2.1
168	-6.23	-0.1	3.0	33.6	8.4	0.5	1.3	35.2	9.3	0.5	1.6	10.6	3.3	3.4	0.5
167	-6.24	0.1	17.5	19.3	21.2	0.1	7.7	17.7	20.3	0.1	7.4	3.8	1.4	1.4	0.1
166	-6.64	0.7	5.7	6.6	32.1	2.6	6.9	6.5	32.2	2.6	6.9	16.2	4.8	4.8	0.5
165	-6.68	3.4	13.2	11.4	4.3	0.3	0.5	11.5	4.2	0.3	0.4	52.0	13.5	13.6	13.8
164	-6.69	0.5	0.4	5.1	3.6	0.2	0.5	5.1	3.6	0.2	0.5	81.7	3.4	3.4	71.8

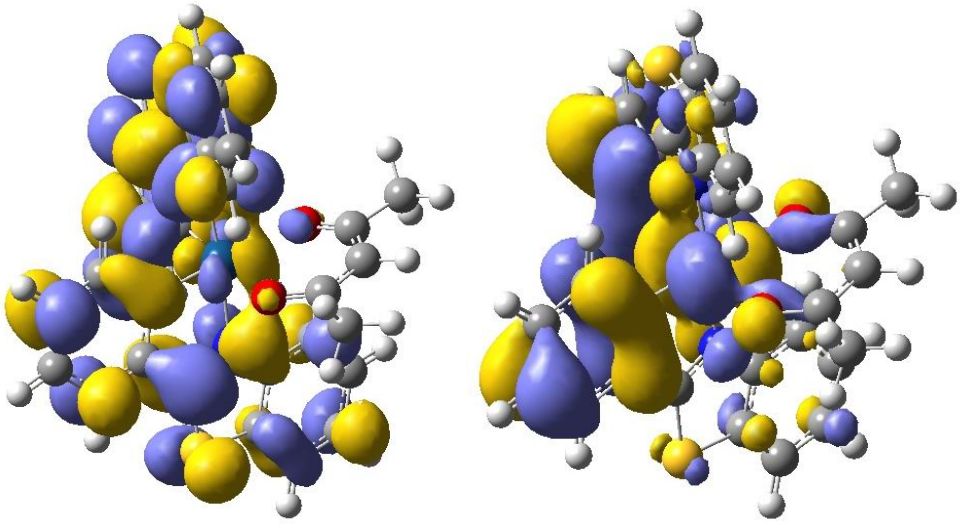

S-Fig. 5 The contour plots of LUMO (left) and HOMO (right) in **(bt)$_2$Ir(acac)** from DFT calculations.

S-Table 2. Molecular orbital compositions (Percent) in the ground state for **(bt)$_2$Ir(acac)** at the B3LYP.

	Orb.	Ir			bt				bt			acac			
Orb.	Energy (eV)	sp	d	ben	total	N	S	ben	total	N	S	total	O	O	C
154	0.42	0.6	1.0	36.3	12.7	0.9	0.4	36.2	12.8	1.0	0.4	0.4	0.1	0.1	0.2
153	0.25	1.4	2.0	10.4	36.8	1.8	13.1	10.8	38.0	1.9	13.2	0.6	0.2	0.2	0.3
152	0.24	2.0	2.7	8.8	39.1	3.3	0.1	8.5	38.0	3.2	0.1	0.8	0.2	0.2	0.4
151	0.11	2.5	2.6	8.3	38.7	1.5	18.9	8.3	38.9	1.5	19.1	0.8	0.2	0.2	0.4
150	0.03	0.9	9.3	2.4	42.6	1.2	29.0	2.4	42.2	1.2	28.7	0.3	0.1	0.1	0.1
149	-0.26	1.1	0.0	0.0	47.6	0.0	2.3	0.1	50.5	0.0	2.4	0.7	0.0	0.0	0.7
148	-0.28	0.4	0.1	1.2	50.0	0.0	2.0	1.2	47.0	0.0	1.9	0.2	0.0	0.0	0.2
147	-0.71	0.1	1.6	0.2	0.9	0.0	0.0	0.2	0.9	0.0	0.0	96.2	12.3	12.3	71.7
146	-1.60	0.8	2.2	13.6	26.6	4.7	3.2	19.0	37.3	6.5	4.5	0.4	0.1	0.1	0.2
145(LUMO)	-1.60	0.6	2.6	**18.7**	**37.3**	6.3	4.6	**13.3**	**26.6**	4.5	3.3	0.9	0.3	0.3	0.3
144(HOMO)	-5.02	0.6	**41.5**	**21.9**	4.9	1.7	0.7	**21.9**	4.9	1.7	0.7	4.3	1.8	1.8	0.7
143	-5.37	0.1	35.0	2.9	4.8	1.3	0.7	3.0	4.8	1.3	0.7	49.3	11.4	11.4	26.5
142	-5.81	0.3	2.0	19.2	18.7	4.5	0.2	19.3	18.8	4.5	0.2	21.6	3.5	3.5	14.7
141	-5.85	0.8	44.2	10.5	14.5	3.5	0.8	10.4	14.5	3.4	0.8	5.1	1.6	1.6	1.8
140	-6.18	0.3	13.3	20.9	10.5	0.2	4.4	20.9	10.6	0.2	4.4	23.5	4.3	4.3	15.0
139	-6.21	0.2	22.3	19.3	18.6	0.3	6.0	19.3	18.6	0.3	6.0	1.6	0.2	0.2	1.1
138	-6.37	0.3	5.5	27.4	16.2	0.3	6.2	27.4	16.2	0.3	6.1	6.9	1.5	1.5	3.9
137	-6.56	-0.1	2.0	14.2	0.3	0.1	0.0	14.2	0.3	0.1	0.0	69.1	23.6	23.6	21.9
136	-6.67	0.2	16.7	1.5	38.6	2.4	5.6	1.5	38.6	2.4	5.6	2.8	0.7	0.7	1.4
135	-6.86	0.1	23.1	2.9	30.9	1.2	2.2	2.9	30.9	1.2	2.2	9.2	0.6	0.6	8.0

X-ray Crystallography: Diffraction data were collected on a Rigaku R-AXIS RAPID diffractometer (Mo Kα radiation, graphite monochromator) in the Ψ rotation scan mode. The structure determination was done with direct methods by using SHELXTL 5.01v and refinements with full-matrix least squares on F^2. The positions of hydrogen atoms were calculated and refined isotropically. **CCDC 725335** (***(bt)$_2$Ir(dipba)***) contains the supplementary crystallographic data for this paper. These data can be obtained free of charge from The Cambridge Crystallographic Data Centre via www.ccdc.cam.ac.uk/data_request/cif.

S-Table 3. Crystal data and structure refinement for **(bt)$_2$Ir(dipba)**.

Identification code	(bt)$_2$Ir(dipba)
Empirical formula	C_{39} H_{35} Ir N_4S_2
Formula weight	816.03
Temperature, K	293(2)
Wavelength, Å	0.71073
Crystal system	Monoclinic,
space group	P2(1)/n
Unit cell dimensions	
a (Å)	8.9808(18)
b (Å)	16.334(3)
c (Å)	22.781(5)
α (deg)	90
β(deg)	90.39(3)
γ (deg)	90
Volume, Å^3	3341.7(12)
Z	4
Calculated density, g/cm^3	1.622
Abs coeff, mm^{-1}	4.355
F(000)	1624
Crystal size, mm	0.20 x 0.17 x 0.16
Theta range for data collection, deg.	3.07 to 27.48
Limiting indices	-11<=h<=9, -21<=k<=21, -29<=l<=29
Reflections collected / unique	31262 / 7588 [R(int) = 0.0476]
Refinement method	Full-matrix least-squares on F^2
Data / restraints / parameters	7588 / 0 / 419
GOF on F^2	0.952
Final R indices [I>2sigma(I)]	R1 = 0.0316, wR2 = 0.0826
R indices (all data)	R1 = 0.0423, wR2 = 0.0877

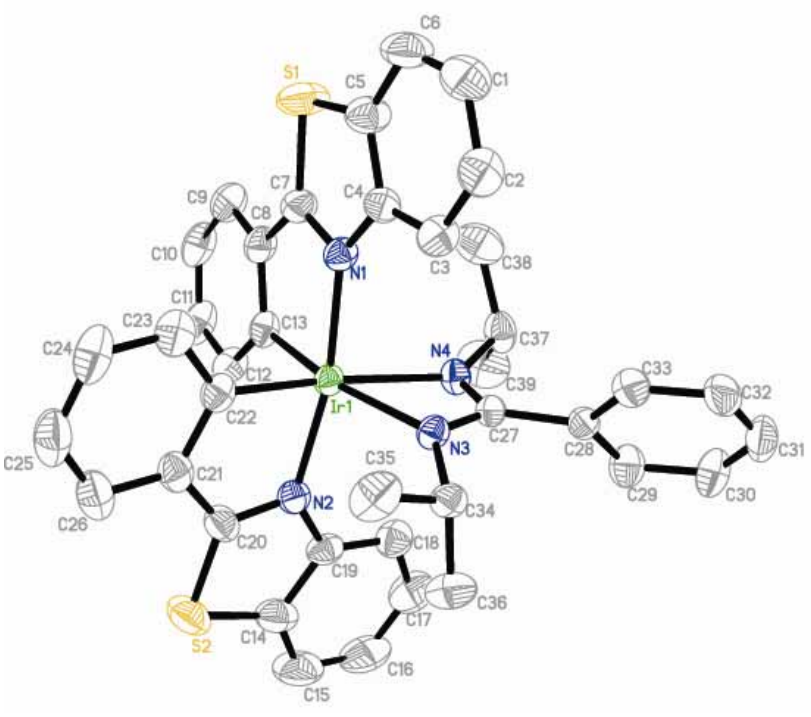

S-Fig. 6 Thermal ellipsoid (ORTEP) plot of **(bt)$_2$Ir(dipba)**.

S-Table 4. Atomic coordinates (x 10^4) and equivalent isotropic displacement parameters (Å^2 x 10^3) for **(bt)$_2$Ir(dipba)**. U(eq) is defined as one third of the trace of the orthogonalized Uij tensor.

	x	y	z	U(eq)
C(1)	7573(7)	5030(4)	1592(3)	55(2)
C(2)	7648(6)	5857(4)	1714(3)	47(1)
C(3)	6495(5)	6381(3)	1556(2)	38(1)
C(4)	5258(5)	6057(3)	1274(2)	32(1)
C(5)	5206(6)	5218(3)	1151(3)	43(1)
C(6)	6377(7)	4698(4)	1304(3)	54(2)
C(7)	2981(6)	5981(3)	852(2)	37(1)
C(8)	1567(5)	6315(3)	669(2)	35(1)
C(9)	366(6)	5835(4)	482(2)	44(1)
C(10)	-952(6)	6231(4)	333(2)	45(1)
C(11)	-1043(6)	7070(4)	367(2)	46(1)
C(12)	150(6)	7535(3)	561(2)	39(1)
C(13)	1501(5)	7173(3)	731(2)	30(1)

C(14)	1240(7)	10100(3)	934(3)	47(1)
C(15)	306(8)	10687(4)	1175(3)	66(2)
C(16)	-239(8)	10553(4)	1729(3)	65(2)
C(17)	147(7)	9861(4)	2043(3)	59(2)
C(18)	1080(6)	9276(4)	1810(2)	43(1)
C(19)	1606(5)	9392(3)	1249(2)	35(1)
C(20)	2845(6)	9138(3)	413(2)	37(1)
C(21)	3755(6)	8643(3)	33(2)	37(1)
C(22)	4092(5)	7874(3)	283(2)	33(1)
C(23)	4967(6)	7355(4)	-66(2)	43(1)
C(24)	5483(7)	7601(5)	-611(2)	53(2)
C(25)	5140(7)	8365(5)	-838(2)	57(2)
C(26)	4246(7)	8884(4)	-519(2)	49(1)
C(27)	4218(5)	7925(3)	2195(2)	28(1)
C(28)	4800(5)	8007(3)	2807(2)	29(1)
C(29)	3992(6)	8405(4)	3240(2)	41(1)
C(30)	4507(7)	8435(4)	3815(2)	50(1)
C(31)	5853(7)	8083(4)	3962(2)	48(1)
C(32)	6688(7)	7701(3)	3541(3)	46(1)
C(33)	6168(6)	7667(3)	2965(2)	39(1)
C(34)	6130(5)	8785(3)	1739(2)	31(1)
C(35)	7010(7)	8759(4)	1175(3)	52(2)
C(36)	5479(7)	9634(4)	1842(3)	52(2)
C(37)	2054(6)	7084(3)	2464(2)	40(1)
C(38)	2045(8)	6190(4)	2275(3)	61(2)
C(39)	468(8)	7390(5)	2504(4)	68(2)
Ir(1)	3313(1)	7689(1)	1100(1)	26(1)
N(1)	3973(4)	6478(2)	1098(2)	30(1)
N(2)	2530(4)	8856(2)	939(2)	31(1)
N(3)	4964(4)	8161(2)	1720(2)	27(1)
N(4)	2932(4)	7585(2)	2054(2)	30(1)
S(1)	3532(2)	4969(1)	812(1)	57(1)
S(2)	2059(2)	10078(1)	249(1)	54(1)

S-Table 5. Bond lengths [Å] and angles [°] for **$(bt)_2$Ir(dipba)**.

C(1)-C(6)	1.367(9)	C(21)-C(22)	1.411(7)
C(1)-C(2)	1.379(9)	C(22)-C(23)	1.406(7)
C(1)-H(1)	0.9300	C(22)-Ir(1)	2.015(5)
C(2)-C(3)	1.389(7)	C(23)-C(24)	1.387(8)
C(2)-H(2)	0.9300	C(23)-H(23)	0.9300
C(3)-C(4)	1.385(7)	C(24)-C(25)	1.385(9)
C(3)-H(3)	0.9300	C(24)-H(24)	0.9300
C(4)-C(5)	1.399(7)	C(25)-C(26)	1.377(9)
C(4)-N(1)	1.400(6)	C(25)-H(25)	0.9300
C(5)-C(6)	1.394(7)	C(26)-H(26)	0.9300
C(5)-S(1)	1.735(5)	C(27)-N(4)	1.319(6)
C(6)-H(6)	0.9300	C(27)-N(3)	1.333(6)
C(7)-N(1)	1.327(6)	C(27)-C(28)	1.493(6)
C(7)-C(8)	1.441(7)	C(28)-C(29)	1.390(7)
C(7)-S(1)	1.728(5)	C(28)-C(33)	1.393(7)
C(8)-C(9)	1.399(7)	C(29)-C(30)	1.386(7)
C(8)-C(13)	1.408(7)	C(29)-H(29)	0.9300
C(9)-C(10)	1.389(8)	C(30)-C(31)	1.378(8)
C(9)-H(9)	0.9300	C(30)-H(30)	0.9300
C(10)-C(11)	1.375(8)	C(31)-C(32)	1.372(9)
C(10)-H(10)	0.9300	C(31)-H(31)	0.9300
C(11)-C(12)	1.384(7)	C(32)-C(33)	1.391(7)
C(11)-H(11)	0.9300	C(32)-H(32)	0.9300
C(12)-C(13)	1.402(7)	C(33)-H(33)	0.9300
C(12)-H(12)	0.9300	C(34)-N(3)	1.461(6)
C(13)-Ir(1)	2.012(5)	C(34)-C(35)	1.512(7)
C(14)-C(15)	1.390(9)	C(34)-C(36)	1.524(7)
C(14)-C(19)	1.399(7)	C(34)-H(34)	0.9800
C(14)-S(2)	1.730(6)	C(35)-H(35A)	0.9600
C(15)-C(16)	1.374(10)	C(35)-H(35B)	0.9600
C(15)-H(15)	0.9300	C(35)-H(35C)	0.9600
C(16)-C(17)	1.381(10)	C(36)-H(36A)	0.9600
C(16)-H(16)	0.9300	C(36)-H(36B)	0.9600
C(17)-C(18)	1.380(8)	C(36)-H(36C)	0.9600
C(17)-H(17)	0.9300	C(37)-N(4)	1.474(6)
C(18)-C(19)	1.378(7)	C(37)-C(39)	1.513(9)
C(18)-H(18)	0.9300	C(37)-C(38)	1.523(8)
C(19)-N(2)	1.401(6)	C(37)-H(37)	0.9800
C(20)-N(2)	1.317(6)	C(38)-H(38A)	0.9600

C(20)-C(21)	1.442(7)	C(38)-H(38B)	0.9600
C(20)-S(2)	1.730(5)	C(38)-H(38C)	0.9600
C(21)-C(26)	1.394(7)	C(39)-H(39A)	0.9600
C(39)-H(39B)	0.9600	C(12)-C(13)-Ir(1)	129.4(4)
C(39)-H(39C)	0.9600	C(8)-C(13)-Ir(1)	115.1(3)
Ir(1)-N(3)	2.182(4)	C(15)-C(14)-C(19)	120.4(6)
Ir(1)-N(4)	2.208(4)	C(15)-C(14)-S(2)	129.2(5)
Ir(1)-N(1)	2.064(4)	C(19)-C(14)-S(2)	110.3(4)
Ir(1)-N(2)	2.065(4)	C(16)-C(15)-C(14)	118.3(6)
		C(16)-C(15)-H(15)	120.9
C(6)-C(1)-C(2)	121.4(5)	C(14)-C(15)-H(15)	120.9
C(6)-C(1)-H(1)	119.3	C(15)-C(16)-C(17)	121.1(6)
C(2)-C(1)-H(1)	119.3	C(15)-C(16)-H(16)	119.5
C(1)-C(2)-C(3)	121.1(5)	C(17)-C(16)-H(16)	119.5
C(1)-C(2)-H(2)	119.5	C(18)-C(17)-C(16)	121.2(6)
C(3)-C(2)-H(2)	119.5	C(18)-C(17)-H(17)	119.4
C(4)-C(3)-C(2)	118.6(5)	C(16)-C(17)-H(17)	119.4
C(4)-C(3)-H(3)	120.7	C(19)-C(18)-C(17)	118.3(6)
C(2)-C(3)-H(3)	120.7	C(19)-C(18)-H(18)	120.8
C(3)-C(4)-C(5)	119.5(4)	C(17)-C(18)-H(18)	120.8
C(3)-C(4)-N(1)	127.0(5)	C(18)-C(19)-C(14)	120.6(5)
C(5)-C(4)-N(1)	113.5(4)	C(18)-C(19)-N(2)	126.1(5)
C(6)-C(5)-C(4)	121.5(5)	C(14)-C(19)-N(2)	113.3(5)
C(6)-C(5)-S(1)	128.2(5)	N(2)-C(20)-C(21)	118.4(4)
C(4)-C(5)-S(1)	110.2(4)	N(2)-C(20)-S(2)	114.7(4)
C(1)-C(6)-C(5)	117.9(6)	C(21)-C(20)-S(2)	126.9(4)
C(1)-C(6)-H(6)	121.1	(26)-C(21)-C(22)	123.2(5)
C(5)-C(6)-H(6)	121.1	C(26)-C(21)-C(20)	124.6(5)
N(1)-C(7)-C(8)	118.5(5)	C(22)-C(21)-C(20)	112.2(4)
N(1)-C(7)-S(1)	114.6(4)	C(23)-C(22)-C(21)	115.3(5)
C(8)-C(7)-S(1)	126.8(4)	C(23)-C(22)-Ir(1)	129.1(4)
C(9)-C(8)-C(13)	123.8(5)	C(21)-C(22)-Ir(1)	115.6(4)
C(9)-C(8)-C(7)	123.5(5)	C(24)-C(23)-C(22)	121.6(6)
C(13)-C(8)-C(7)	112.7(4)	C(24)-C(23)-H(23)	119.2
C(10)-C(9)-C(8)	117.8(5)	C(22)-C(23)-H(23)	119.2
C(10)-C(9)-H(9)	121.1	C(25)-C(24)-C(23)	121.3(6)
C(8)-C(9)-H(9)	121.1	C(25)-C(24)-H(24)	119.4
C(11)-C(10)-C(9)	120.1(5)	C(23)-C(24)-H(24)	119.4
C(11)-C(10)-H(10)	119.9	C(26)-C(25)-C(24)	119.2(6)
C(9)-C(10)-H(10)	119.9	C(26)-C(25)-H(25)	120.4
C(10)-C(11)-C(12)	121.3(5)	C(24)-C(25)-H(25)	120.4
C(10)-C(11)-H(11)	119.4	C(25)-C(26)-C(21)	119.4(6)
C(12)-C(11)-H(11)	119.4	C(25)-C(26)-H(26)	120.3

C(11)-C(12)-C(13)	121.5(5)	C(21)-C(26)-H(26)	120.3
C(11)-C(12)-H(12)	119.2	N(4)-C(27)-N(3)	111.6(4)
C(13)-C(12)-H(12)	119.2	N(4)-C(27)-C(28)	124.4(4)
C(12)-C(13)-C(8)	115.4(4)	N(3)-C(27)-C(28)	123.9(4)
C(29)-C(28)-C(33)	117.8(4)	C(37)-C(38)-H(38A)	109.5
C(29)-C(28)-C(27)	121.6(4)	C(37)-C(38)-H(38B)	109.5
C(33)-C(28)-C(27)	120.6(4)	H(38A)-C(38)-H(38B)	109.5
C(30)-C(29)-C(28)	121.0(5)	C(37)-C(38)-H(38C)	109.5
C(30)-C(29)-H(29)	119.5	H(38A)-C(38)-H(38C)	109.5
C(28)-C(29)-H(29)	119.5	H(38B)-C(38)-H(38C)	109.5
C(31)-C(30)-C(29)	120.1(5)	C(37)-C(39)-H(39A)	109.5
C(31)-C(30)-H(30)	119.9	C(37)-C(39)-H(39B)	109.5
C(29)-C(30)-H(30)	119.9	H(39A)-C(39)-H(39B)	109.5
C(32)-C(31)-C(30)	120.1(5)	C(37)-C(39)-H(39C)	109.5
C(32)-C(31)-H(31)	119.9	H(39A)-C(39)-H(39C)	109.5
C(30)-C(31)-H(31)	119.9	H(39B)-C(39)-H(39C)	109.5
C(31)-C(32)-C(33)	119.8(5)	C(13)-Ir(1)-C(22)	87.82(19)
C(31)-C(32)-H(32)	120.1	C(13)-Ir(1)-N(1)	80.16(17)
C(33)-C(32)-H(32)	120.1	C(22)-Ir(1)-N(1)	92.29(18)
C(32)-C(33)-C(28)	121.2(5)	C(13)-Ir(1)-N(2)	92.24(17)
C(32)-C(33)-H(33)	119.4	C(22)-Ir(1)-N(2)	79.44(18)
C(28)-C(33)-H(33)	119.4	N(1)-Ir(1)-N(2)	169.04(14)
N(3)-C(34)-C(35)	109.6(4)	C(13)-Ir(1)-N(3)	164.35(17)
N(3)-C(34)-C(36)	111.3(4)	C(22)-Ir(1)-N(3)	107.82(16)
C(35)-C(34)-C(36)	111.0(5)	N(1)-Ir(1)-N(3)	98.45(15)
N(3)-C(34)-H(34)	108.3	N(2)-Ir(1)-N(3)	90.98(14)
C(35)-C(34)-H(34)	108.3	C(13)-Ir(1)-N(4)	104.40(17)
C(36)-C(34)-H(34)	108.3	C(22)-Ir(1)-N(4)	167.71(17)
C(34)-C(35)-H(35A)	109.5	N(1)-Ir(1)-N(4)	88.63(15)
C(34)-C(35)-H(35B)	109.5	N(2)-Ir(1)-N(4)	100.98(15)
H(35A)-C(35)-H(35B)	109.5	N(3)-Ir(1)-N(4)	59.95(14)
C(34)-C(35)-H(35C)	109.5	C(7)-N(1)-C(4)	111.7(4)
H(35A)-C(35)-H(35C)	109.5	C(7)-N(1)-Ir(1)	113.3(3)
H(35B)-C(35)-H(35C)	109.5	C(4)-N(1)-Ir(1)	134.9(3)
C(34)-C(36)-H(36A)	109.5	C(20)-N(2)-C(19)	111.8(4)
C(34)-C(36)-H(36B)	109.5	C(20)-N(2)-Ir(1)	114.2(3)
H(36A)-C(36)-H(36B)	109.5	C(19)-N(2)-Ir(1)	133.6(3)
C(34)-C(36)-H(36C)	109.5	C(27)-N(3)-C(34)	122.9(4)
H(36A)-C(36)-H(36C)	109.5	C(27)-N(3)-Ir(1)	94.6(3)
H(36B)-C(36)-H(36C)	109.5	C(34)-N(3)-Ir(1)	138.5(3)
N(4)-C(37)-C(39)	111.3(5)	C(27)-N(4)-C(37)	123.4(4)
N(4)-C(37)-C(38)	110.9(5)	C(27)-N(4)-Ir(1)	93.8(3)
C(39)-C(37)-C(38)	109.3(5)	C(37)-N(4)-Ir(1)	138.8(3)

N(4)-C(37)-H(37)	108.4	C(7)-S(1)-C(5)	90.0(2)
C(39)-C(37)-H(37)	108.4	C(20)-S(2)-C(14)	89.9(3)
C(38)-C(37)-H(37)	108.4		

S-Table 6. Anisotropic displacement parameters ($Å^2$ x 10^3) for **$(bt)_2Ir(dipba)$**. The anisotropic displacement factor exponent takes the form: $-2\pi^2[h^2 a^{*2}U^{11} + ... + 2 h k a^* b^* U^{12}]$

	U11	U22	U33	U23	U13	U12
C(1)	46(3)	53(4)	65(4)	1(3)	-8(3)	20(3)
C(2)	33(3)	58(4)	51(3)	-4(3)	-6(2)	11(3)
C(3)	30(2)	41(3)	44(3)	-5(2)	-2(2)	3(2)
C(4)	28(2)	33(3)	35(2)	0(2)	-1(2)	7(2)
C(5)	36(3)	35(3)	57(3)	-4(2)	-8(2)	4(2)
C(6)	59(4)	33(3)	71(4)	-4(3)	-8(3)	14(3)
C(7)	41(3)	30(3)	39(3)	-4(2)	-8(2)	-2(2)
C(8)	32(2)	40(3)	33(2)	-3(2)	-6(2)	-5(2)
C(9)	42(3)	47(3)	43(3)	-9(2)	-10(2)	-9(2)
C(10)	31(3)	65(4)	39(3)	-13(3)	-6(2)	-14(3)
C(11)	30(3)	66(4)	40(3)	-15(3)	-5(2)	6(2)
C(12)	32(3)	43(3)	41(3)	-10(2)	-6(2)	7(2)
C(13)	24(2)	40(3)	27(2)	-4(2)	-2(2)	3(2)
C(14)	50(3)	32(3)	58(3)	1(2)	-5(3)	4(2)
C(15)	77(5)	33(3)	86(5)	-2(3)	-9(4)	17(3)
C(16)	62(4)	43(4)	88(5)	-22(3)	1(4)	15(3)
C(17)	59(4)	57(4)	61(4)	-17(3)	12(3)	7(3)
C(18)	42(3)	44(3)	43(3)	-4(2)	-1(2)	5(2)
C(19)	30(2)	29(2)	45(3)	-6(2)	-7(2)	3(2)
C(20)	39(3)	36(3)	36(2)	6(2)	-5(2)	1(2)
C(21)	33(3)	42(3)	34(2)	3(2)	-6(2)	-1(2)
C(22)	27(2)	39(3)	33(2)	-4(2)	-4(2)	0(2)
C(23)	34(3)	54(3)	40(3)	-3(2)	-1(2)	6(2)
C(24)	41(3)	83(5)	36(3)	-13(3)	1(2)	4(3)
C(25)	60(4)	78(5)	33(3)	2(3)	5(3)	-15(3)
C(26)	50(3)	61(4)	36(3)	9(3)	-2(3)	-8(3)
C(27)	30(2)	26(2)	27(2)	0(2)	-6(2)	0(2)
C(28)	28(2)	28(2)	30(2)	2(2)	-4(2)	-4(2)
C(29)	38(3)	52(3)	34(2)	-1(2)	2(2)	2(2)
C(30)	52(3)	66(4)	31(3)	-10(3)	-1(2)	0(3)
C(31)	55(3)	56(4)	32(3)	4(2)	-12(2)	-15(3)
C(32)	46(3)	42(3)	49(3)	8(2)	-19(3)	-4(3)

C(33)	40(3)	37(3)	39(3)	1(2)	-5(2)	1(2)
C(34)	27(2)	30(2)	35(2)	0(2)	-2(2)	-5(2)
C(35)	42(3)	58(4)	56(3)	-10(3)	16(3)	-19(3)
C(36)	58(4)	34(3)	65(4)	-5(3)	6(3)	-7(3)
C(37)	37(3)	51(3)	31(2)	8(2)	-1(2)	-13(2)
C(38)	66(4)	47(4)	70(4)	17(3)	10(3)	-16(3)
C(39)	50(4)	72(5)	81(5)	12(4)	26(4)	-9(3)
Ir(1)	25(1)	27(1)	26(1)	-1(1)	-3(1)	0(1)
N(1)	28(2)	30(2)	32(2)	-3(2)	-3(2)	0(2)
N(2)	30(2)	31(2)	33(2)	-1(2)	-7(2)	2(2)
N(3)	25(2)	30(2)	28(2)	-2(2)	-1(2)	-3(2)
N(4)	28(2)	36(2)	27(2)	2(2)	-2(2)	-2(2)
S(1)	56(1)	30(1)	84(1)	-12(1)	-24(1)	2(1)
S(2)	65(1)	41(1)	57(1)	16(1)	-3(1)	9(1)

***S-reference*:**

S1 E. Runge, E. K. U. Gross, *Phys. Rev. Lett.* 1984, **52**, 997.

S2 A. D. Becke, *J. Chem. Phys.* 1993, **98**, 5648.

S3 (a) P. J. Hay, W. R. Wadt, *J. Chem. Phys.* 1985, **82**, 270. (b) P. J. Hay, W. R. Wadt, *J. Chem. Phys.* 1985, **82**, 299.

S4 (a) M. E. Casida, C. Jamorski, K. C. Casida, D. R. Salahub, *J. Chem. Phys.* 1998, **108**, 4439. (b) R. E. Stratmann, G. E. Scuseria, M. J. Frisch, *J. Chem. Phys.* 1998, **109**, 8218. (c) N. N. Matsuzawa,; A. Ishitani, D. A. Dixon, T. Uda, *J. Phys. Chem. A* 2001, **105**, 4953.

S5 (a) V. Barone, M. Cossi, J. Tomasi, *J. Chem. Phys.* 1997, **107**, 3210. (b) M. Cossi, G. Scalmani, N. Rega, V. Barone, *J. Chem. Phys.* 2002, **117**, 43.

S6 (a) J. E. Monat, J. H. Rodriguez, J. K. McCusker, *J. Phys. Chem. A* 2002, **106**, 7399. (b) X. Zhou, H. X. Zhang, Q. J. Pan, B. H. Xia, A. C. Tang, *J. Phys. Chem. A* 2005, **109**, 8809. (c) T. Liu, B. H. Xia, X. Zhou, H. X. Zhang, Q. J. Pan, J. S. Gao, *Organometallics* 2007, **26**, 143. (d) T. Liu, H. X. Zhang, B. H. Xia, *J. Phys. Chem. A* 2007, **111**, 8724.

S7 M. J. Frisch,; G. W. Trucks, H. B. Schlegel, G. E. Scuseria, M. A. Robb, J. R. Cheeseman, J. A. Montgomery , T. Vreven, K. N. Kudin, J. C. Burant, J. M. Millam, S. S. Iyengar, J. Tomasi, V. Barone, B. Mennucci, M. Cossi, G. Scalmani, N. Rega, G. A. Petersson, H. Nakatsuji, M. Hada, M. Ehara, K. Toyota, R. Fukuda, J. Hasegawa, M. Ishida, T. Nakajima, Y. Honda, O. Kitao, H. Nakai, M. Klene, X. Li, J. E. Knox, H. P. Hratchian, J. B. Cross, C. Adamo, J. Jaramillo, R. Gomperts, R. E. Stratmann, O. Yazyev, A. J. Austin, R. Cammi, C. Pomelli, J. W. Ochterski, P. Y. Ayala, K. Morokuma, G. A. Voth, P. Salvador, J. J. Dannenberg, V. G. Zakrzewski, S. Dapprich, A. D. Daniels, M. C. Strain, O. Farkas, D. K. Malick, A. D. Rabuck, K. Raghavachari, J. B. Foresman, J. V. Ortiz, Q. Cui, A. G. Baboul, S. Clifford, J. Cioslowski, B. B. Stefanov, G. Liu, A.

Liashenko, P. Piskorz, I. Komaromi, R. L. Martin, D. J. Fox, T. Keith, M. A. Al-Laham, C. Y. Peng, A. Nanayakkara, M. Challacombe, P. M. W. Gill, B. Johnson, W. Chen, M. W. Wong, C. Gonzalez, J. A. Pople, *Gaussian 03, Revision C.02. Gaussian, Inc.: Pittsburgh, PA* 2003.